J Fluoresc (2015) 25:247–251
DOI 10.1007/s10895-014-1500-2

ORIGINAL PAPER

Preparation and Fluorescence Properties of Crystalline Gel Rare Earth Phosphates

Hiroaki Onoda · Takehiro Funamoto

Received: 14 August 2014 / Accepted: 11 December 2014 / Published online: 28 January 2015

Abstract An aqueous solution of sodium dihydrogen phosphate was mixed with a aqueous solution of lanthanum nitrate and stirred for 24 h, and the pH was adjusted to 11 using ammonia. The obtained phosphates were analyzed using X-ray diffraction, Fourier transform infrared spectroscopy, thermogravimetry–differential thermal analysis, and scanning electron microscopy. The lanthanum phosphate gel was obtained with a large amount of water. The fluorescence of the gels was investigated by substituting a part of the lanthanum cations with cerium, terbium, and europium cations. UV–vis reflectance and fluorescence spectra of these substituted materials were obtained and analyzed. Rrare-earth phosphate gels with large amounts of water exhibited bluish purple, green, and red fluorescence when cation ratios of La/Ce=70/30, La/Ce/Tb=55/30/15, and La/Eu=95/5 were used, respectively.

Keywords Gel material · Rare earth phosphate · pH control · Fluorescence

Introduction

Recently, fluorescent materials have been used in various types of applications, including lights, displays, biolabels, and paints. White light-emitting diodes are important because of the high energy they emit and the absence of mercury in their structures [1]. White light-emitting diodes are obtained by mixing three-color fluorescence (blue, green and red) to form white light. Currently, nitrides and oxides are used as fluorescent materials [2, 3]. Attempts have also been made to use other inorganic compounds for the synthesis of fluorescent materials targeting various applications [4].

Rare-earth phosphates have high melting points and large specific surface areas [5, 6]. Rare-earth orthophosphates, which are the main components of rare-earth metal ores, are stable in acidic and basic solutions, and this property was used to improve the acid/base resistance of other phosphate materials [7]. Moreover, rare-earth metals have important fluorescence properties. Specifically, europium-containing compounds have been reported to exhibit strong fluorescence in various materials [8].

Although gels, by weight, are mostly liquid, they behave like solid, jelly-like materials. Gels consist of three-dimensional cross-linked networks, and their strength varies from soft and weak to hard and strong. Various processes have been established to synthesize gel materials, including the use of natural gelling agents, polymer gelling agents, and inorganic gelling agents such as metal alkoxides. Metal alkoxides are useful inorganic gelling agents for sol–gel processes [9–12]. However, these compounds are expensive, harmful, and difficult to handle.

Herein, lanthanum phosphate gels were synthesized from lanthanum nitrate and sodium dihydrogen phosphate. The respective chemical compositions and particle shapes of the obtained products were evaluated. Their fluorescence properties were investigated by substituting a portion of the lanthanum cations with cerium, terbium, and europium cations. The UV–vis reflectance and fluorescence spectra of these substituted materials were obtained and analyzed.

Experimental

A aqueous solution of sodium dihydrogen phosphate (NaH_2PO_4) (0.04 mol/L) was mixed with a aqueous solution of 0.04 mol/L of lanthanum nitrate, and stirred for 24 h. The

H. Onoda (✉) · T. Funamoto
Department of Informatics and Environmental Sciences, Kyoto Prefectural University, 1-5, Shimogamo Nakaragi-cho, Sakyo-ku, Kyoto 606-8522, Japan
e-mail: onoda@kpu.ac.jp

solution pH was adjusted to 11 using ammonia. When the resulting solution was left to stand for a few hours and the pH was lowered to pH 9 by itself, a gel material was formed, which was filtered off. The fluorescence spectra were investigated by replacing a portion of the lanthanum cations with cerium, terbium, and europium cations using the corresponding nitrates. Gel materials were synthesized with cation ratios of La/Ce=70/30, La/Ce/Tb=55/30/15, and La/Eu=95/5 [13, 14]. The respective chemical compositions of the obtained gel materials were analyzed using X-ray diffraction (XRD), Fourier transform infrared spectroscopy (FT-IR), and thermogravimetry-differential thermal analysis (TG-DTA). XRD patterns were recorded on a Rigaku Denki MiniFlex X-ray diffractometer (Rigaku Corp., Akishima, Japan) using monochromated CuKα radiation (scan step; 0.02°, scan speed; 3°/min, Vertical goniometer). The IR spectra were recorded on a HORIBA FT-IR 720 (Horiba Ltd., Kyoto, Japan) using the KBr disk method. The TG and DTA curves were measured using a Shimadzu DTG-60A system (Shimadzu Corp., Kyoto Japan) at a heating rate of 10 °C/min, under air. The particle shapes of the phosphate powder were investigated using scanning electron microscopy (SEM, JGM-5510LV; JEOL Ltd., Akishima, Japan, accelerating voltage; 15 kV). The samples were analyzed using ultraviolet–visible (UV–Vis) reflectance with the help of a UV2100 system (Shimadzu Corp., Kyoto Japan). The fluorescence properties were measured using a luminescence spectrometer (LS55; Perkin-Elmer, Waltham, Massachusetts, USA).

Results and Discussion

Chemical Compositions and Particle Shapes of Lanthanum Phosphate

Figure 1 shows the XRD patterns of the samples prepared at pH 11. The characteristic peaks of Rhabdophane-type lanthanum orthophosphate, $LaPO_4\ nH_2O$ (n=0.5–2), were observed in the XRD patterns [15, 16]. This crystal structure contains vacant spaces in which the crystallization water can move freely. Figure 2 shows the IR spectra of samples prepared at pH 11. The absorption peaks at 3400 and 1630 cm^{-1} were attributed to the adsorbed water and water of crystallization. The peaks at 1380 and 3200 cm^{-1} were attributed to nitrate anions. The peaks at 1050, 610, and 540 cm^{-1} were attributed to phosphate anions [17]. These results corresponded with those obtained using XRD.

The undried sample suffered over 95 % weight loss. Therefore, the samples were dried for 24 h, and then analyzed by TG-DTA. Figure 3 shows the TG-DTA curves of the samples. The DTA curve presents two endothermic peaks: a large one at 80 °C and another at 250 °C. These peaks were due to the volatilization of adsorbed water and elimination of the water of crystallization. The TG curve presents two weight loss events at these temperatures. The amount of water of crystallization present, n, was 1.25, calculated from the weight loss. By analyzing the XRD and TG-DTA curves, the chemical composition of the dried sample was determined to be $LaPO_4\ 1.25H_2O$. Because the original gel material suffered more than 95 % weight loss upon drying, the amount of adsorbed water was found to be in large excess as compared to the water of crystallization.

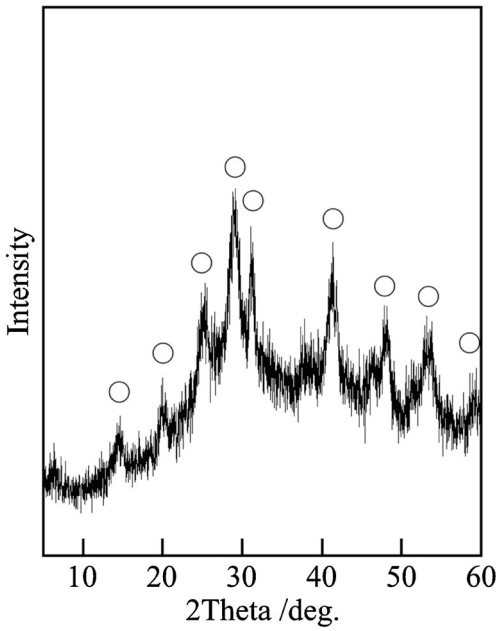

Fig. 1 XRD pattern of the gel sample prepared from lanthanum nitrate and sodium dihydrogen phosphate solution, at pH 11, ○, $LaPO_4 \cdot nH_2O$

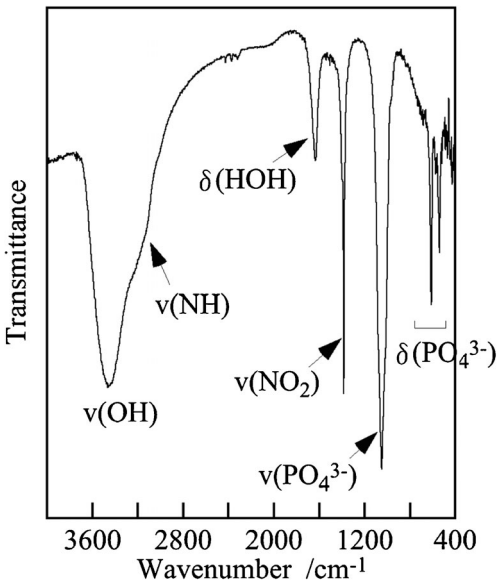

Fig. 2 IR spectrum of gel sample prepared from lanthanum nitrate and sodium dihydrogen phosphate solution at pH 11

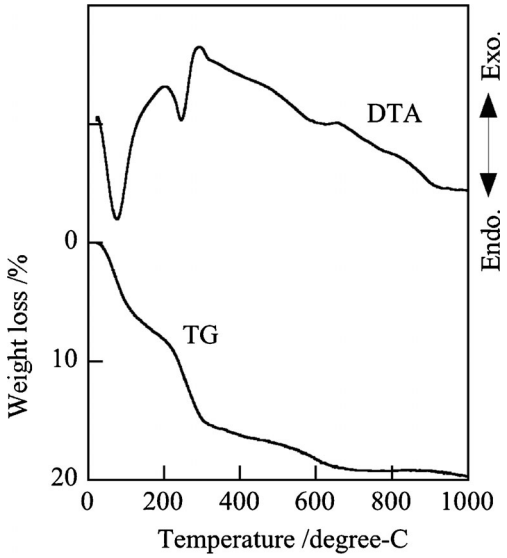

Fig. 3 TG-DTA curves of the sample after drying for 24 h

Figure 4 depicts the SEM images of the dispersed solution and gel materials. The dispersed solution contained small angular particles (Fig. 4a). The particle size was found to be 2–3 μm at the long end and 1–2 μm at the short end, with a thickness of 0.5 μm. From the SEM images (Fig. 4b), we can see that the gel material has a flat surface. The phosphate gel grows from the small angular particles when the solution pH is adjusted to 11.

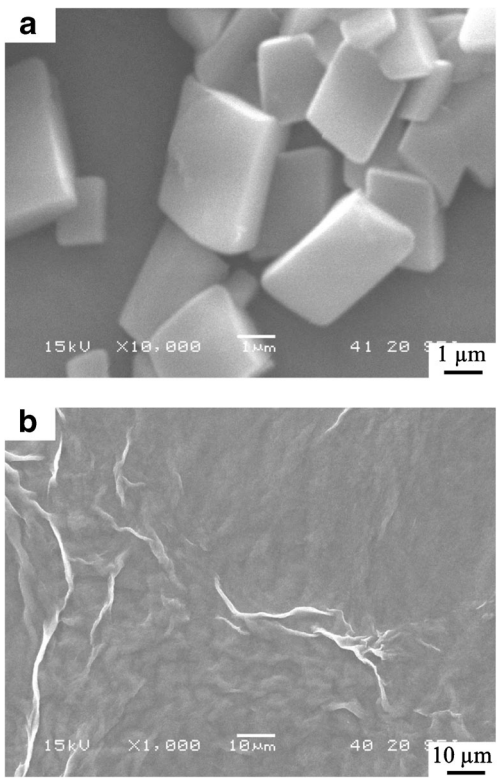

Fig. 4 SEM images of samples: **a** dispersed solution and **b** gel material

Although the formation mechanism of the gel material could not be clarified, some important factors influencing the final structure can be taken into consideration. The Rhabdophane-type starting structure mentioned above is important because it contains the pore sites. On the pore sites of the Rhabdophane-type structure, a hydrogen-bond network is formed with the ammonium cations. This network also contains a large amount of water. As mentioned above, 95 % weight loss occurred after drying. The major part of this weight loss was due to the volatilization of water. Excess ammonia was found to be important for gel formation, because the use of a small amount of ammonia did not afford the gel material.

Fluorescence Properties of Phosphate Materials

The fluorescence properties were investigated by substituting a part of the lanthanum cations in the lanthanum phosphate gel with cerium, terbium, and europium cations. Herein, gel materials were obtained at cation ratios of La/Ce=70/30, La/Ce/Tb=55/30/15, and La/Eu=95/5. Because cerium phosphate forms Rhabdophane-type structures similar to those formed by lanthanum phosphate, we also obtained cerium–lanthanum phosphate gels. In contrast, in the case of the terbium and europium phosphates, the Rhabdophane-type structure was difficult to form. Further, terbium phosphate did not form gel materials. Thus, we can conclude that the formation of gel materials is directly related to the formation of Rhabdophane-type structures. Because the terbium concentration in La/Ce/Tb=55/30/15 and the europium concentration in La/Eu=95/5 are quite small, these compounds can form gel materials.

Figure 5 shows the UV–vis reflectance spectra of samples prepared using various ratios of rare-earth metals. All samples showed high reflectance at visible wavelengths. An absorbance peak at 215 nm was observed in the spectrum of the lanthanum phosphate gel (Fig. 5a). This absorbance corresponds with the bandgap of lanthanum phosphate (5.8 eV). The reflectance spectra of the samples prepared with cation ratios of La/Ce=70/30 and La/Ce/Tb=55/30/15 had an absorption peak at 320 nm because of the Ce^{3+} 5d–4f transition (Fig. 5b and c) [18]. The adsorption peak at 230 nm in the spectrum of the sample prepared with a cation ratio of La/Ce/Tb=55/30/15 corresponds to the Tb^{3+} 5d–4f transition (Fig. 5c) [13]. The adsorption peak at 250 nm in the spectrum of the sample prepared with a cation ratio of La/Eu=95/5 corresponds to the Eu^{3+}–O^{2-} charge transfer (Fig. 5d) [19]. Absorbance peaks due to each chemical composition were observed despite the large amount of water in the gel materials.

Figure 6 shows the excitation and emission spectra of the sample prepared with a cation ratio of La/Ce=70/30. The emission and excitation wavelengths were 380 and 254 nm,

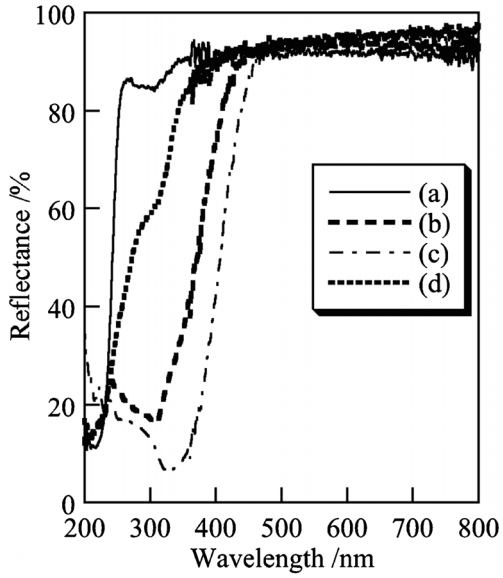

Fig. 5 UV–vis reflectance spectra of samples, **a** La, **b** La/Ce=70/30, **c** La/Ce/Tb=55/30/15, and **d** La/Eu=95/5

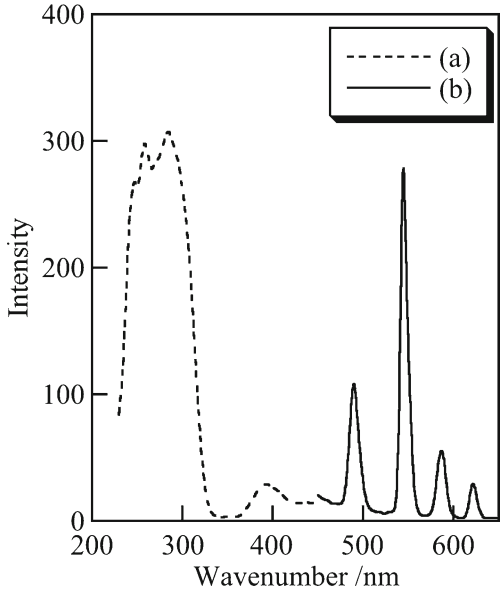

Fig. 7 Excitation (**a**) and emission (**b**) spectra of sample prepared at La/Ce/Tb=55/30/15

respectively. Wide peaks were observed in the excitation and emission spectra, due to the f–d transition. The peak at 248 nm in the excitation spectrum corresponds to the charge-transfer band from O^{2-} to Ce^{3+}. The peaks at 260 and 282 nm correspond to the Ce^{3+} 4f–5d transition from $^2F_{5/2}$ to $^2D_{5/2}$ and $^2D_{3/2}$, respectively. In the emission spectrum, the peaks at 380 and 425 nm correspond to the Ce^{3+} 4f–5d transition from $^2D_{3/2}$ to $^2F_{5/2}$ and $^2F_{7/2}$, respectively [13, 18, 20]. The emission light of this material was strong near the ultraviolet range. Because the human eye cannot readily perceive ultraviolet light, the sample seemed to exhibit bluish-purple fluorescence.

Figure 7 shows the excitation and emission spectra of the sample prepared with a cation ratio of La/Ce/Tb=55/30/15. The emission and excitation wavelengths were 545 and 254 nm, respectively. The peak at 248 nm in the excitation spectrum corresponds to the charge-transfer band from O^{2-} to Ce^{3+}. The peaks at 260 and 282 nm correspond to the Ce^{3+} 4f–5d transition from $^2F_{5/2}$ to $^2D_{5/2}$ and $^2D_{3/2}$, respectively. The peak at 390 nm corresponds to the Tb^{3+} f–f transition from $^7F_6$ to $^5D_3$, respectively. In the emission spectrum, the peaks at 490, 545, 580, and 625 nm correspond to the Tb^{3+} f–f transition from $^5D_4$ to $^7F_6$, $^7F_5$, $^7F_3$, and $^7F_2$, respectively [13, 14, 21, 22]. Because the Tb^{3+} cation exhibits no absorbance between 260 and 280 nm, its fluorescence is weak. When a

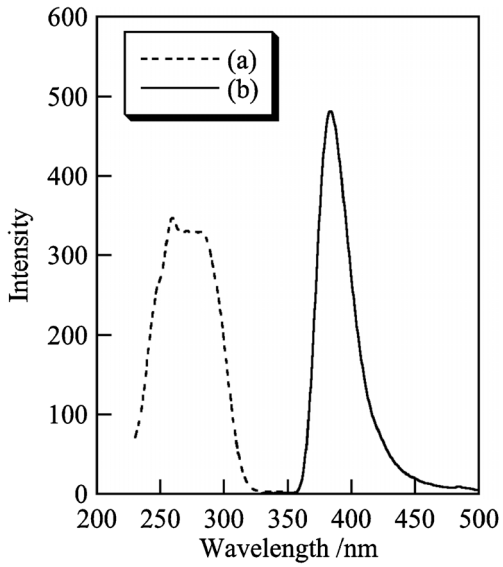

Fig. 6 Excitation (**a**) and emission (**b**) spectra of sample prepared at La/Ce=70/30

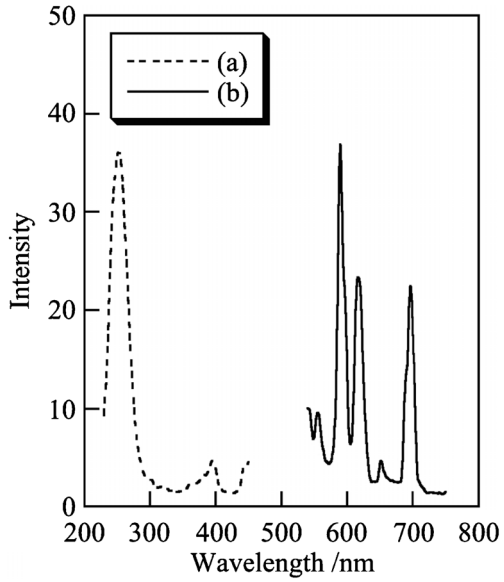

Fig. 8 Excitation (**a**) and emission (**b**) spectra of sample prepared at La/Eu=95/5

cerium cation is added, there is energy transfer from Ce^{3+}(f–d) to Tb^{3+}(f–f), and the fluorescence becomes strong. Because the 545 nm emission is dominant, the samples exhibited green fluorescence.

Figure 8 shows the excitation and emission spectra of the sample prepared with a cation ratio of La/Eu=95/5. The emission and excitation wavelengths were 592 and 254 nm, respectively. The peaks at 250 and 395 nm in the excitation spectrum correspond to the charge-transfer band of the O^{2-} to Eu^{3+} and Eu^{3+} f–f transitions from $^7F_0$ to $^5L_6$, respectively. The peaks at 558, 589, 612, 650, and 695 nm in the emission spectrum correspond to the Eu^{3+} f–f transition from $^5D_0$ to $^7F_0$, $^7F_1$, $^7F_2$, $^7F_3$, and $^7F_4$, respectively [13, 20–22]. Because the emission at 590 nm is dominant, the samples exhibited red fluorescence.

Generally, water-containing materials exhibit weak fluorescence. However, the gel materials obtained in this work contained a large amount of water, yet showed strong fluorescence. Rare-earth phosphate gels with large amounts of water and with cation ratios of La/Ce=70/30, La/Ce/Tb=55/30/15, and La/Eu=95/5, exhibited bluish-purple, green, and red fluorescence, respectively.

Conclusions

Lanthanum phosphate gels with large amounts of water were synthesized from lanthanum nitrate and sodium dihydrogen phosphate. The chemical composition of the sample was Rhabdophene-type lanthanum phosphate, as demonstrated using XRD analysis. Rare-earth phosphate gels exhibited bluish-purple, green, and red fluorescence when cation ratios of La/Ce=70/30, La/Ce/Tb=55/30/15, and La/Eu=95/5 were used, respectively. The materials synthesized in this work are promising candidates for novel fluorescence materials that can be used under high-moisture conditions.

References

1. Ye S, Xiao F, Pan YX, Ma YY, Zhang QY (2010) Mater Sci Eng R Rep 71(1):1–34
2. Lei W, Portehault D, Dimova R, Antonietti M (2011) J Am Chem Soc 133(18):7121–7127
3. Som S, Choubey A, Sharma SK (2012) Phys B Condens Matter 407(17):3515–3519
4. Toda A, Uematsu K, Ishigaki T, Toda K, Sato M (2010) Mater Sci Eng B 173(1–3):168–170
5. Rajesh K, Shajesh P, Seidei O, Mukundan P, Warrier KGK (2007) Adv Funct Mater 17(10):1682–1690
6. Onoda H, Taniguchi K, Tanaka I (2008) Microporous Mesoporous Mater 109(1–3):193–198
7. Onoda H, Matsui H, Tanaka I (2007) Mater Sci Eng B 141(1–2):28–33
8. Bettinelli M, Piccinelli F, Speghini A, Ueda J, Tanabe S (2012) J Lumin 132(1):27–29
9. Qiao Y, Lin Y, Zhang S, Huang J (2011) Chem Eur J 17(18):5180–5187
10. Smirnov VA, Sukhadolski GA, Philippova OE, Khokhlov AR (1999) J Phys Chem B 103(36):7621–7626
11. Lee SH, Teshima K, Shikine N, Oishi S (2009) Cryst Growth Des 9(9):4078–4083
12. Huang CC, Lo YW, Kuo WS, Hwu JR, Su WC, Shieh DB, Yeh CS (2008) Langmuir 24(15):8309–8313
13. Yang M, You HP, Liu K, Zheng Y, Guo N, Zhang HJ (2010) Inorg Chem 49(11):4996–5002
14. Liviano SR, Aparicio FJ, Rojas TC, Hungria AB, Chinchilla LE, Ocana M (2012) Cryst Growth Des 12(2):635–645
15. Ramesh K, Zheng J, Ling EGY, Han YF, Borgna A (2009) J Phys Chem C 113(37):16530–16537
16. Mooney RCL (1950) Acta Crystallogr 3(5):337–340
17. Corbridge DEC, Lowe EJ (1954) J Chem Soc 493:4555–4564
18. Guan MY, Sun J, Shang TM, Zhou Q, Han J, Ji A (2010) J Meter Sci Technol 26(1):45–48
19. Dorman JA, Choi JH, Kuzmanich G, Chang JP (2012) J Phys Chem C 116(23):12854–12860
20. Li G, Chao K, Peng H, Chen K, Zhang Z (2008) J Phys Chem C 112(42):16452–16456
21. Yu L, Song HW, Liu ZX, Yang LM, Zheng SLZ (2005) J Phys Chem B 109(23):11450–11455
22. Yang DM, Li GG, Kang XJ, Cheng Z, Ma P, Peng C, Lian HZ, Li CX, Lin J (2012) Nanoscale 4(11):3450–3459